Journal of Neurochemistry, 2005, **93**, 724–736 doi:10.1111/j.1471-4159.2005.03061.x

Constitutive expression and localization of cytochrome P-450 1A1 in rat and human brain: presence of a splice variant form in human brain[1]

Shankar J. Chinta,*,† Reddy P. Kommaddi,* Cheri M. Turman,‡ Henry W. Strobel‡ and Vijayalakshmi Ravindranath*,†

*Division of Cellular and Molecular Neuroscience, National Brain Research Centre, Nainwal Mode, Manesar, Haryana, India
†Department of Neurochemistry, National Institute of Mental Health and Neurosciences, Bangalore, India
‡University of Texas Medical School at Houston, Houston, Texas, USA

Abstract

Cytochrome P-450 function as mono-oxygenases and metabolize xenobiotics. CYP1A1, a cytochrome P-450 enzyme, bioactivates polycyclic aromatic hydrocarbons to reactive metabolite(s) that bind to DNA and initiate carcinogenesis. Northern and immunoblot analyses revealed constitutive expression of Cyp1a1 and CYP1A1 in rat and human brain, respectively. CYP1A1 mRNA and protein were localized predominantly in neurons of cerebral cortex, Purkinje and granule cell layers of cerebellum and pyramidal neurons of CA1, CA2, and CA3 subfields of the hippocampus. RT–PCR analyses using RNA obtained from autopsy human brain samples demonstrated the presence of a splice variant having a deletion of 87 bp of exon 6. This splice variant was present in human brain, but not in the liver from the same individual, and was absent in rat brain and liver. Structural modeling indicated broadening of the substrate access channel in the brain variant. The study demonstrates the presence of a unique cytochrome P-450 enzyme in human brain that is generated by alternate splicing. The presence of distinct cytochrome P-450 enzymes in human brain that are different from well-characterized hepatic forms indicates that metabolism of xenobiotics including drugs could occur in brain by pathways different from those known to occur in liver.

Keywords: brain, CYP1A1, cytochrome P-450, drug metabolism, mono-oxygenases.
J. Neurochem. (2005) **93,** 724–736.

Cytochrome P-450 (P-450) superfamily of heme proteins is involved in metabolism of a vast array of carcinogens, drugs, and endogenous compounds. P-450 enzymes exist in multiple forms and are selectively induced or inhibited by a variety of chemicals. They are known to exist in liver, the major organ involved in P-450-mediated xenobiotic metabolism (de Montellano 1986). However, the importance of extrahepatic metabolism has been increasingly recognized, especially with respect to its potential role in target organ toxicity. This has prompted extensive investigations into the xenobiotic metabolizing capability of extrahepatic organs such as kidney, lung, brain, etc. in laboratory animals and humans (Gram *et al*. 1986). Studies from our laboratory and others have demonstrated the presence of a competent microsomal P-450 system in the rodent (Anandatheerthavarada *et al*. 1990) and human brain (Ravindranath *et al*. 1989), and its ability to metabolize a variety of xenobiotics. Multiple forms of P-450 enzymes, which are selectively induced by 3-methyl cholanthrene, β-naphthoflavone, phenobarbital, and ethanol are expressed in brain (Ravindranath

Received November 24, 2004; revised manuscript received December 20, 2004; accepted December 22, 2004.

Address correspondence and reprint requests to Vijayalakshmi Ravindranath, National Brain Research Centre, Nainwal Mode, Manesar, 122050, Haryana, India. E-mail: vijir@nbrc.ac.in

[1]Individual cytochrome P-450 gene in human is represented as 'CYP' and rat as 'Cyp' followed by an Arabic number denoting family and an alphabetical letter designating subfamily (CYP1A/Cyp1a). An Arabic number is used to represent genes within a subfamily (e.g. human CYP1A1 and rat Cyp1a1). Cytochrome P-450 protein is represented with a prefix 'P-450' (P-450 1A1/P-450 1a1) in a similar manner. When reference is made to both the rat and human forms, CYP1A1 and P-450 1A1 are used.

Abbreviations used: FISH, fluorescence *in situ* hybridization; ML, molecular layer; P-450, cytochrome P-450; PBS, phosphate-buffered saline; SDS–PAGE, sodium dodecyl sulfate polyacrylamide gel electrophoresis.

and Boyd 1995). These studies have also demonstrated the constitutive presence of several forms of P-450 enzymes including 1A1/A2, 2B1/2B2, 2D6, 2E1, and P-450 3A in rat and human brain (Anandatheerthavarada *et al*. 1990; Ravindranath and Boyd 1995). Because brain exhibits regional and cellular heterogeneity it is important to determine the localization of specific forms of P-450 as it would help to understand the potential consequences of metabolism of xenobiotics mediated by specific enzymes of P-450.

Cytochrome P-450 1A1, a member of the P-450 superfamily, is a major extrahepatic enzyme and is induced by administration of 3-methylcholanthrene, β-naphthoflavone (Gozukara *et al*. 1984) or 2,3,7,8-tetra chlorobenzo-p-dioxin (Jones *et al*. 1986). P-450 1A1 contributes notably to the toxicity of many carcinogens, especially polycyclic aromatic hydrocarbons, as it is the principal enzyme that bioactivates the inert hydrocarbons into DNA-binding reactive metabolites (Park *et al*. 1996). The presence of P-450 1A1 in brain could potentially play a role in the initiation of carcinogenesis *in situ,* as polycyclic aromatic hydrocarbons are lipophilic and can cross the blood–brain barrier.

The expression of Cyp1a1 in rat brain (Anandatheerthavarada *et al*. 1990; Morse *et al*. 1998) and CYP1A1 in human brain (Farin and Omiecinski 1993) has been demonstrated using RT–PCR. However, relatively little is known about the regional and cellular localization of P-450 1A1. Recent studies have also shown that induction of the P-450 1A1 enzyme by polycyclic aromatic hydrocarbons increases the generation of reactive oxygen species, which may cause oxidative damage in brain (Strolin-Benedetti *et al*. 1999). Therefore, the present study was undertaken to study the constitutive expression and topographic distribution of this enzyme at the mRNA and protein level in rat and human brain.

Materials and methods

Materials

cDNA to Cyp1a1 was obtained as gift from Dr Avadhani (Univ. of Pennsylvania, Philadelphia, PA, USA). DIG-RNA labeling and detection kit, antidigoxigenin Fab fragments linked to peroxidase and alkaline phosphatase were purchased from Roche Biochemicals (Indianapolis, IN, USA). The tyramide signal amplification kit was obtained from New England Nuclear (Boston, MA, USA) and Vectastain-ABC Elite kit was purchased from Vector Labs (Burlingame, CA, USA). All other chemicals and reagents were of analytical grade and were obtained from Sigma Chemical Company (St Louis, MO, USA) or Qualigens (Bangalore, India).

Animals

Male Wistar rats (3–4 months, 225–250 g) were obtained from the Central Animal Research Facility of the National Institute of Mental Health and Neurosciences. Animals had access to a pelleted diet (Lipton India, Calcutta, India) and water *ad libitium*. All animal experiments were carried out in accordance with the National Institutes of Health guidelines for the care and use of laboratory animals and were approved by the institutional ethics committee. All efforts were made to minimize animal suffering, to reduce number of animals used, and to utilize alternatives to *in vivo* techniques, if available.

Human brain tissue

Human brain tissues were obtained at autopsy from traffic accident victims with no known neurological or psychiatric disorders through the Human Brain Tissue Repository, Department of Neuropathology, NIMHANS. The Human Brain Tissue Repository has been established to provide human post-mortem tissue to researchers in India taking into due consideration all the ethical concerns of the Government of India. Brain tissues from both male and female subjects were used. The average age of the individuals was 24.76 ± 20.22 years and post-mortem delay between death and autopsy was 7.3 ± 3.7 h. After autopsy, brain samples were washed in ice-cold saline and dissected into different regions such as cortex, hippocampus, striatum, midbrain, cerebellum, and thalamus based on standard anatomical markings. All regions were flash-frozen and stored at − 70°C immediately. Regions from each human brain were thawed on ice and used for the preparation of microsomes as described below. Microsomes were aliquoted and stored at − 70°C.

Preparation of microsomes

Animals were anesthetized with ether and perfused transcardially with ice-cold Tris buffer (100 mM, pH 7.4) containing KCl (1.15%, w/v) prior to decapitation and removal of the brain. Rat brain regions (cortex, cerebellum, midbrain, hippocampus, and thalamus) were dissected out using standard anatomical landmarks (Glowinski and Iversen 1966). Rat and human brain regions were homogenized using a Potter–Elvehjem homogenizer in 9 volumes of ice-cold Tris

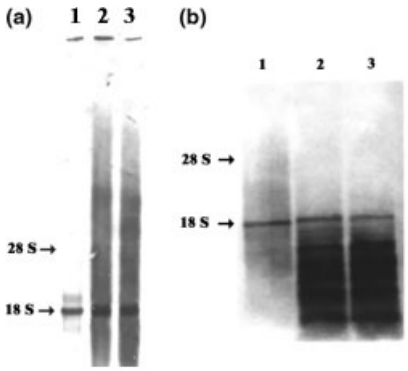

Fig. 1 Northern blot analysis showing the constitutive expression of Cyp1a1 and CYP1A1 mRNA in rat and human brain. Total RNA from rat liver (a, lane1; 3 μg) and poly-(A^+) RNA from rat brain cortex and cerebellum (lane 2–3, 5 μg) and poly-(A^+) RNA from autopsy human brain cortex from three subjects (b, lanes 1–3, 5 μg) were electrophoresed under denaturing conditions. After transfer to nylon membrane, the blots were hybridized with antisense riboprobe prepared using cDNA to Cyp1a1. The mobility of the 18S and 28S ribosomal RNA is indicated. The expression of Cyp1a1 in rat and CYP1A1 in human brain was seen as bands close to the 18S ribosomal RNA which nearly corresponds to the size of 1.6 Kb.

buffer (0.1 mM), EDTA (0.1 mM), KCl (1.15%, w/v), phenyl methyl sulfonyl fluoride (0.1 mM), butylated hydroxytoluene (22 μM), glycerol (20%, v/v), aprotinin (0.001%, w/v), and leupeptin (0.001%, w/v), previously bubbled with nitrogen (buffer A). The homogenate was centrifuged at 17 000 *g* for 30 min at 4°C. Thereafter, the supernatant was centrifuged at 100 000 *g* for 1 h to give the microsomal pellet. The pellet was suspended in a small volume of buffer A, aliquoted, flash-frozen in liquid nitrogen, and stored at − 70°C (Ravindranath and Anandatheerthavarada 1990). The protein concentration was measured by the dye-binding method (Bradford 1976).

Immunoblot analyses

Microsomal proteins from rat (50 μg) and human (50 μg) brain regions were subjected to sodium dodecyl sulfate polyacrylamide gel electrophoresis (SDS–PAGE; Laemmli and Favre 1973). Proteins were transferred from the gel to nitrocellulose membranes (Towbin *et al*. 1979). Membranes were immunostained with antiserum to rat liver P-450 1a1 (Anandatheerthavarada *et al*. 1990) followed by incubation with anti-rabbit IgG labeled with alkaline phosphatase (Vector Laboratories). Immunostained bands were detected using nitroblue tetrazolium and 5-bromo 4-chloro 3-indolyl phosphate as chromogens.

Northern blotting

The cDNA to rat liver Cyp1a1 was used for preparation of riboprobes. Total RNA from rat liver and poly-$(A)^+$RNA from rat brain cortex and cerebellum and human brain cortex were extracted as described by Chomezynski (1993). Total RNA and mRNA were separated electrophoretically and transferred to positively charged nylon membrane by capillary transfer (Kevil *et al*. 1997), UV cross-linked and hybridized with digoxigenin-labeled antisense riboprobe prepared using T7 RNA polymerase to Cyp1a1. Sense cRNA probe was synthesized using SP6 RNA polymerase. Membrane was hybridized overnight with digoxigenin-labeled sense and antisense riboprobe at 50°C, washed, incubated with antibody to digoxigenin

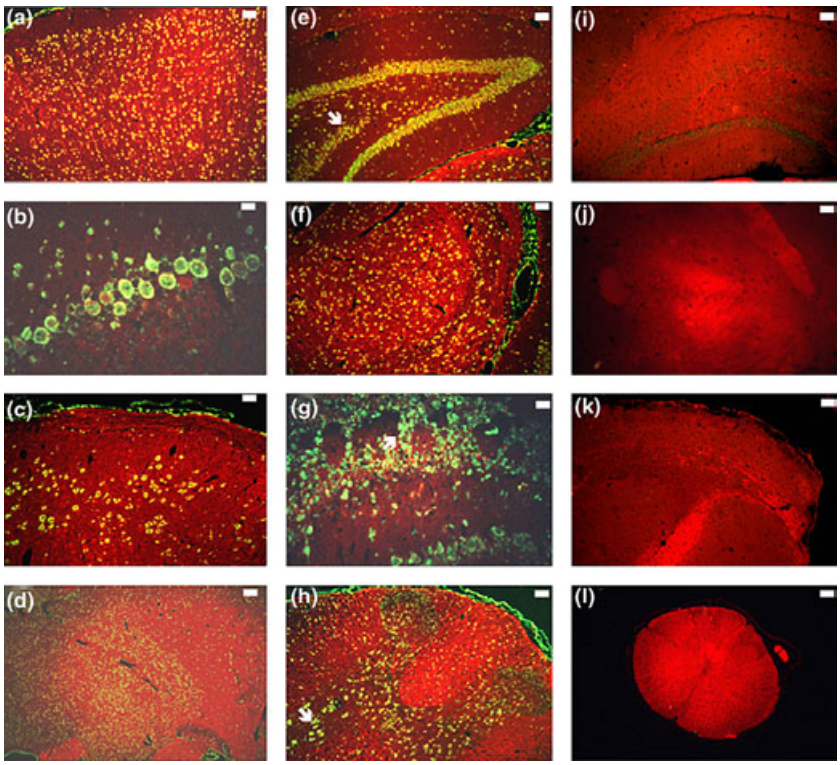

Fig. 2 Localization of Cyp1a1 mRNA in normal rat brain using fluorescent *in situ* hybridization. (a) The presence of Cyp1a1 mRNA in the neurons of cerebral cortex. Bar = 100 μm. (b) Intense fluorescence was seen in the Purkinje neurons of the cerebellum hybridized with antisense probe. Bar = 25 μm. (c) Staining of the reticular neurons in the midbrain showed the expression of the Cyp1a1 mRNA. Bar = 50 μm. (d) Expression of Cyp1a1 mRNA was seen in the neurons of the striatum, although to a lesser extent than the neurons in the cerebral cortex. Bar = 50 μm. (e) The granule cell layer of the dentate gyrus was intensely fluorescent showing the expression of Cyp1a1 mRNA. Intense fluorescence was seen in the CA1 pyramidal cell layer of hippocampus. Staining of CA3 neurons is indicated by the arrow. Bar = 100 μm. (f) Cyp1a1 mRNA was observed in the thalamic neurons. Bar = 25 μm. (g) Intense fluorescence of glomeruli neurons (arrow) shows the expression of Cyp1a1mRNA in the olfactory bulb. Bar = 50 μm. (h) The anterior horn cells of the spinal cord (arrow) were intensely fluorescent indicating the substantial expression of Cyp1a1. Bar = 50 μm. (i) Control section of hippocampus hybridized with the sense probe did not show any FITC fluorescent staining. Bar = 200 μm. (j) The control section of thalamic region hybridized with sense probe did not reveal any FITC staining. Bar = 200 μm. (k) Control section of the olfactory bulb hybridized with the digoxigenin labeled with sense probe counter stained with Evan's blue. Bar = 200 μm. (l) Control section of spinal cord hybridized with the digoxogenin labeled sense probe. Bar = 200 μm.

Fab fragments conjugated with alkaline phosphatase. The bands were visualized using a chromogenic substrate for alkaline phosphatase.

Fluorescence *in situ* hybridization

Male Wistar rats were anesthetized and perfused transcardially with normal saline followed by buffered paraformaldehyde (4%, w/v; 200 mL/rat) prior to the removal of the brain. Different regions of human brain (cortex, cerebellum, hippocampus) obtained at autopsy were dissected out and fixed in buffered paraformaldehyde as above. The tissue was processed for paraffin embedding and serial sections (8–10 μm thick) were cut under RNase-free conditions. Sections were dewaxed, hydrated in graded ethanol, acetylated, and treated with proteinase K. Sections were then rinsed in phosphate-buffered saline (PBS) and dehydrated using graded ethanol. Digoxigenin-labeled antisense and sense cRNA (for control sections) were synthesized from Cyp1a1 cDNA using T7 and SP6 RNA polymerases, respectively. Sections were hybridized overnight at 50°C with sense or antisense probes. After hybridization, sections were washed, incubated with blocking reagent (0.5%, w/v, NEN Life Sciences) and then with antibody to digoxigenin conjugated to horseradish peroxidase. After washing, sections were incubated with biotinylated tyramide followed by streptavidin fluorescein. Finally, sections were washed, dried and counterstained with Evan's Blue prior to examination under a fluorescence microscope.

RT–PCR analysis of RNA from rat and human brain cortex

Total RNA was isolated from brain and liver of rats, human brain cortex, and liver obtained at autopsy as described above. The first strand of cDNA was synthesized using 1 μg of total RNA from human brain, oligo dT primers and reverse transcriptase. The second strand was synthesized using T4 DNA polymerase. Double-stranded DNA was purified by phenol/chloroform

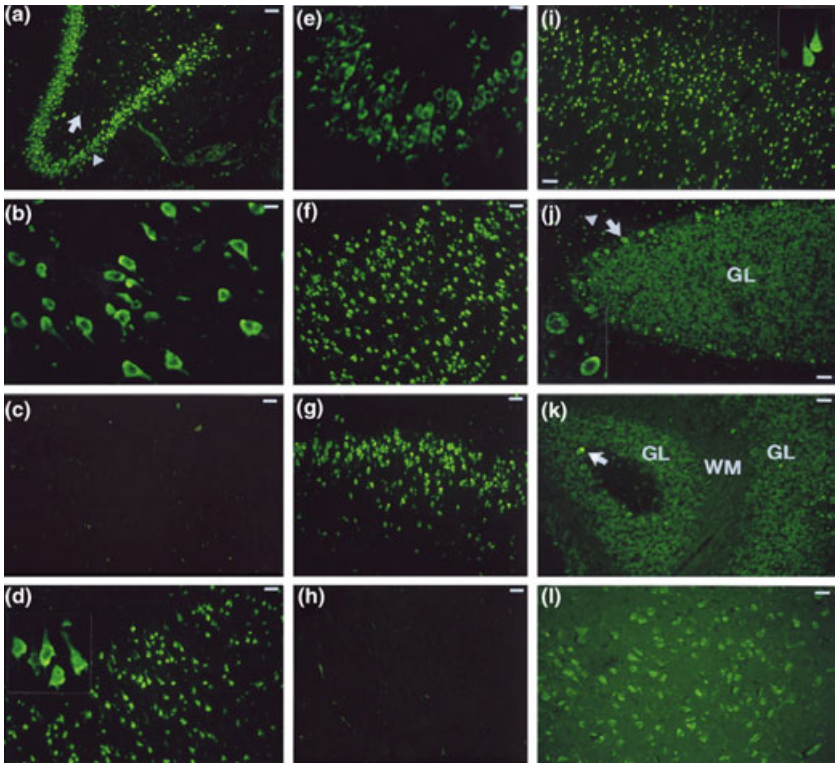

Fig. 3 Localization of CYP1A1 mRNA in human brain by fluorescence *in situ* hybridization. (a) Intense fluorescence was observed in the dentate gyrus (arrowhead) region of the hippocampus. Staining of the interneurons of the hilus (arrow) was also observed. Bar = 100 μm. (b) Higher magnification of CA3 neurons shows the expression of CYP1A1 mRNA in the hippocampus. Bar = 25 μm. (c) The control section hybridized with sense probe. Bar = 100 μm. (d) The presence of CYP1A1 mRNA in the pyramidal neurons of the CA1 subfield in the hippocampus. Inset: Higher magnification of CA1 neurons. (e) Higher magnification of the granule cells in the dentate gyrus. Bar = 25 μm. (f) Intense fluorescence was seen in the CA3 pyramidal cell layers of the human brain. Bar = 100 μm. (g) Robust staining of the CA2 pyramidal cell layer of the human brain shows the presence of CYP1A1 in human brain. (h) Similar section of hippocampus hybridized with the sense probe. Bar = 100 μm. (i) Intense fluorescence was seen in neuronal cell layers of the human brain frontal cortex. Differential fluorescence was seen delineating the laminar architecture of the cortex. Inset shows the higher magnification of cortical neurons. Bar = 200 μm. (j) Fluorescent labeling of the Purkinje cells (arrow) and the granule cell layer (GL) in human cerebellum indicating the presence of CYP1A1 mRNA. Sparse staining of the cells in the molecular layer (ML) was also noted. Bar = 100 μm. Higher magnification of a Purkinje neuron is shown in the inset. (k) Another view of cerebellum showing the expression of CYP1A1. The arrow shows the labeling of Purkinje neurons. Neurons in the granule cell layer (GL) were also stained. Bar = 200 μm. (l) Sparse staining was observed in the reticular neurons of the midbrain region. Bar = 200 μm.

extraction and alcohol precipitation and then used as template for PCR. The primers used for amplification of CYP1A1 (GenBank Accession No. K03191) were 5′- to 3′-TGGATGAGAACGCCA-ATGTC (representing bases from 967 to 986) and 5′- to 3′-TGGGTTGACCCATAGCTTCT (representing bases from 1358 to 1339) and expected size of the PCR product was 392. cDNA synthesized from 1 μg of total RNA was suspended in 5 μL of 10 mM Tris–HCl (pH 8.3) and added to the final reaction mixture which contained 50 mM KCl, 200 μM of each dNTP, $MgCl_2$ (2.5–3.5 mM), primers (80–85 pmole), and 0.25 units of AmpliTaq DNA polymerase. The thermal cycling conditions used for CYP1A1 were as follows: initial denaturation at 94°C for 5 min followed by 40 cycles consisting of 30 s at 94°C, 30 s at 60°C and 60 s at 72°C with a final extension at 72°C for 2 min. Negative control consisted of sterile water instead of template DNA. The PCR products (20 μL) were separated by electrophoresis using 1.2% agarose gel and stained with ethidium bromide. The identity of PCR products was confirmed by sequencing. The following primers, forward 5′- CACATCCGGGACATCACAG-3′ (representing bases from 913 to 931) and reverse 5′-GTCTCCCC-AATGCACTTTCG-3′ (representing bases from 1447 to 1466) were used to amplify the region exon 3–7 of rat brain and liver Cyp1a1 cDNA (GenBank Accession No. NM_012540). The anticipated size of the amplicon is 554 bp.

Immunohistochemistry

Paraffin-embedded sections of rat and human brain were prepared as described above. Sections were dewaxed and transferred to PBS containing hydrogen peroxide (3% v/v) to block the endogenous peroxidase reaction. The sections were pressure cooked in sodium citrate buffer (0.01 M, pH 6) for antigen retrieval, blocked with normal goat serum and incubated with antiserum to P-450 1a1 (Anandatheerthavarada *et al*. 1990). Control sections were incubated with non-immune serum. The sections were washed, treated with biotinylated anti-rabbit IgG, and incubated with VECTASTAIN-Elite ABC reagent. Color was developed, using diaminobenzidine and hydrogen peroxide. The sections were washed in water, dehydrated in graded ethanol, cleared with xylene, dried, and mounted in Permont.

Homology modeling of human brain variant P-450 1A1

The homology models of human brain variant P-450 1A1 and liver P-450 1A1 were constructed using mammalian CYP2C5 bound to 4-methyl-*N*-methyl-*N*-(2-phenyl-2H-pyrazol-3-yl)benzenesulfonamide (DMZ) crystal structure coordinates (1 N6B) as template (Wester *et al*. 2003). Unlike the original CYP2C5 PDB file (1DT6), this template does contain coordinates for the FG loop region. Alignments followed that of Szklarz and Paulsen (2002, Fig. 9) and MODELLER (Sali and Blundell 1993) was used for generation of the models. Ten models were generated for each protein and the best as determined by inspection and PROCHECK (Laskowski *et al*. 1993) were chosen for further molecular dynamic simulations. Psfgen utility within NAMD (Kalé *et al*. 1999) using CHARMM22 forcefield parameters allowed creation of psf and pdb files needed for simulations. The models were solvated with water using the program VMD (Humphrey *et al*. 1996) and coordinates transferred back to NAMD for energy minimization and simulated annealing. Particle Mesh Ewald (PME) algorithm was used to deal with long-range electrostatics using a grid size of $80 \times 80 \times 80$. A dielectric constant of 1 was used. The systems were minimized for 20 000 steps using the conjugate gradient method. The simulated annealing protocol followed minimization by rapidly heating the systems to 550 K in 6 ps and maintaining at 550K for an additional 6 ps. They were slowly allowed to cool from 550 K to 0 K in 24 ps. All figures were generated with Swiss PDB Viewer and rendered for publication quality in POVRAY 3.5 (Guex and Peitsch 1997).

Results

Northern blot analysis of Cyp1a1/CYP1A1 expression in rat and human brain

Northern blot analysis of mRNA from rat brain cortex and cerebellum, and human brain cortex from three subjects using the cDNA to Cyp1a1 revealed the constitutive expression of CYP1A1 mRNA in both rat and human brain. The relative mobility of the transcript was similar to 18S ribosomal RNA (depicted by arrow in Figs 1a and b). The relative size of 18S rRNA is approximately 1.6 kb. This was similar to that seen in rat liver (Fig. 1a).

Localization of Cyp1a1 mRNA in rat brain by fluorescence *in situ* hybridization

Fluorescence *in situ* hybridization (FISH) studies demonstrated the presence of Cyp1a1 mRNA predominantly in neuronal cells in rat brain regions when hybridized with the riboprobe synthesized from the cDNA to Cyp1a1. High levels of Cyp1a1 mRNA expression were seen in olfactory bulb, thalamus, cerebral cortex, and hippocampus. The neurons in the cerebral cortex showed intense cytosolic staining, indicating the presence of Cyp1a1 mRNA

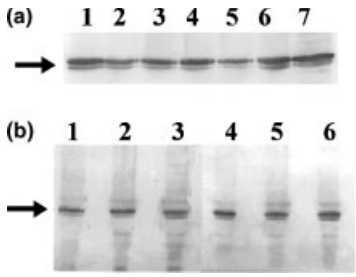

Fig. 4 Immunoblot analysis of microsomal protein from rat (a) and human (b) brain regions stained with antiserum to brain P-450 1a1. Microsomal protein (50 μg) prepared from rat (a) and human (b) brain regions were subjected to SDS–PAGE followed by immunoblotting onto nitrocellulose membrane with antiserum to P-450 1a1. (a) The lanes contained microsomal protein from rat brain cortex (lane 1), cerebellum (lane 2), brain stem (lane 3), hippocampus (lane 4), striatum (lane 5), thalamus (lane 6), and whole brain (lane 7). (b) Immunostained bands were also detectable in microsomes from human brain regions such as striatum (lane 1), thalamus (lane 2), hipocampus (lane 3), cortex (lane 4), cerebellum (lane 5), and midbrain (lane 6).

(Fig. 2a). The laminar architecture of different cortical layers was clearly seen in the sections hybridized with antisense probe. In the cerebellum, Purkinje cells showed intense fluorescence, while interneurons of the molecular layer (ML) were relatively less stained (Fig. 2b). In midbrain, the reticular neurons were selectively labeled, indicating the predominant presence of Cyp1a1 mRNA within this cell population (Fig. 2c). There was only sparse staining of neurons in the striatum (Fig. 2d), whereas control sections hybridized with sense probe did not show any fluorescence (data not shown). Intense fluorescence was seen in hippocampus in the pyramidal neurons of CA1 and CA2 and in granule cell layer in the dentate gyrus (Fig. 2e). The control sections hybridized with the sense probe did not show any fluorescence (Fig. 2i). Thalamic neurons were stained intensely showing expression of Cyp1a1 mRNA (Fig. 2f). The corresponding control sections hybridized with sense probe are shown in Fig. 2(j). In olfactory lobe, neurons in glomeruli were intensely labeled (Fig. 2g). The anterior horn cells of the spinal cord were intensely fluorescent, indicating expression of Cyp1a1 mRNA (Fig. 2h), whereas control sections, olfactory and spinal cord, hybridized with the sense probe did not show any fluorescence (Figs 2k and l). All sections were counter stained with Evan's Blue.

Localization of CYP1A1 mRNA in human brain by FISH

FISH studies demonstrated the presence of CYP1A1 mRNA predominantly in neuronal cells in the human brain regions. The granule cells in dentate gyrus (Figs 3a

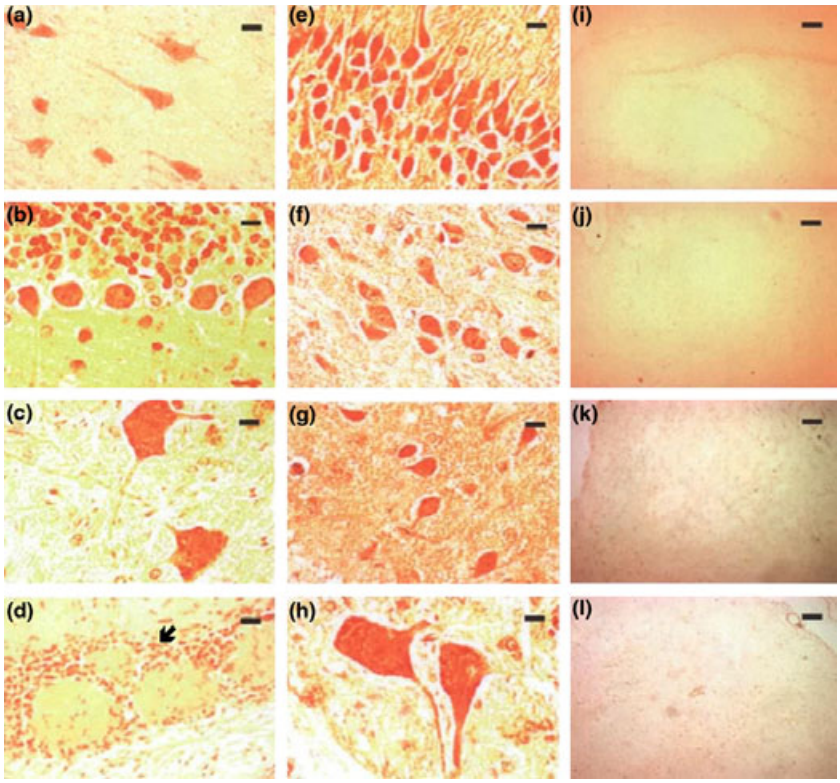

Fig. 5 Localization of P-450 1a1 in rat brain by immunohistochemistry. Immunostaining of cortical neurons in rat brain showing the expression of P-450 1a1 protein. Intense labeling of apical dendrites was observed in the cortical neurons. Bar = 10 μm. (b) Immunostaining of the granule cell layer of cerebellum was seen. Higher magnification of cerebellum showing intense staining in Purkinje cells indicating the presence of P-450 1a1. Bar = 10 μm. (c) Intense immunostaining of reticular neurons in midbrain showing the presence of P-450 1a1 in rat brain. Bar = 10 μm. (d) Immunostaining was observed in the neurons of glomeruli (arrow) demonstrating the presence of the P-450 1a1 protein. Bar = 200 μm. (e) Immunostaining was seen in the CA1 pyramidal neurons of the hippocampus indicating the presence of P-450 1a1 protein. The axonal processes of neurons were labeled intensely. Bar = 10 μm. (f) Expression of P-450 1a1 seen in the neurons of thalamus. Bar = 10 μm. (g) Intense staining of striatal neurons observed when rat brain sections were treated with P-450 1a1 antiserum. Bar = 10 μm. (h) Intense immunostaining was seen in anterior horn cells of spinal cord for P-450 1a1 antiserum. Bar = 10 μm. (i) Control section of hippocampus treated with non-immune serum did not show any staining. Bar = 200 μm. (j) No staining was seen in similar section of thalamic region incubated with non-immune serum. Bar = 200 μm. (k) No staining was observed in striatal section incubated with non-immune serum. Bar = 200 μm. (l) Control section of spinal cord incubated with pre-immune serum did not show any staining. Bar = 200 μm.

and e) and pyramidal neurons in CA3 region of hippocampus were stained (Figs 3b and f), while control sections hybridized with sense probe did not show any fluorescence (Figs 3c and h). Pyramidal neurons in CA1 (Fig. 3d) and CA2 (Fig. 3g) were intensely stained. High levels of CYP1A1 mRNA were seen in neuronal cells in frontal cortex (Fig. 3i). In the cerebellum, Purkinje cells and the granule cell layer showed significant fluorescence (Figs 3j and k). Occasional staining was seen in the molecular layer. In the midbrain, reticular neurons were stained, although not as intensely as seen in the cerebellum and cortex (Fig. 3l). Thus, there was specific neuronal labeling while other cell populations did not show any fluorescence indicating the selective localization of CYP1A1 mRNA in human brain.

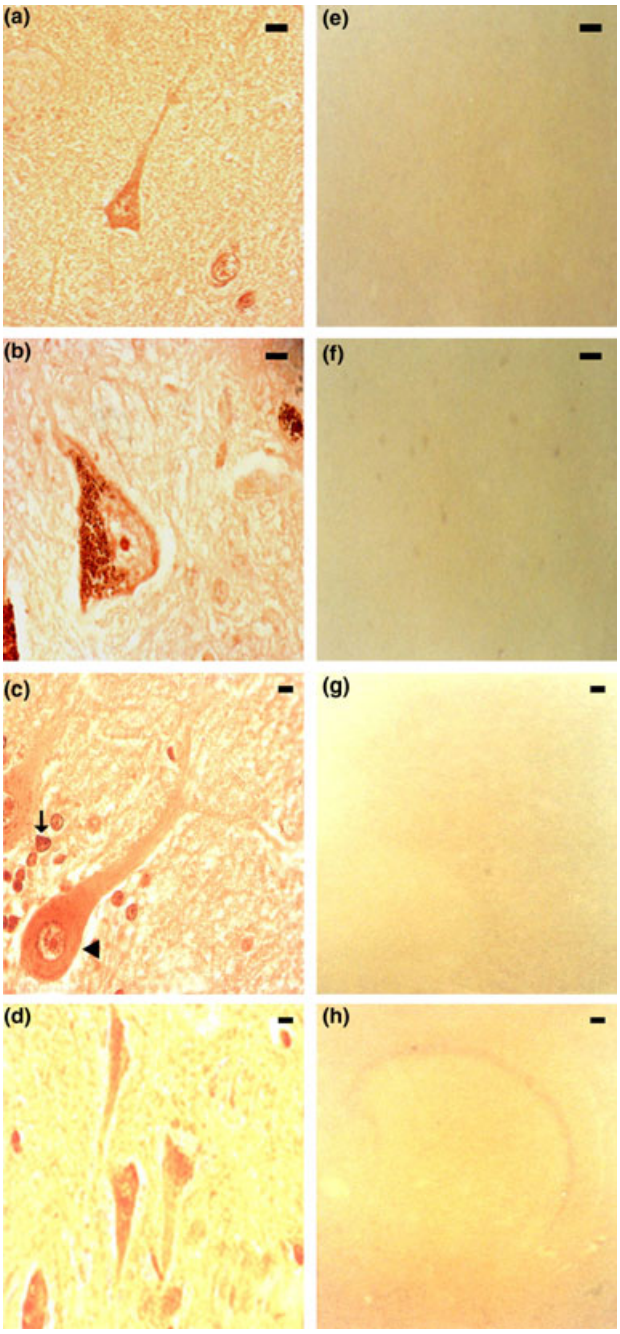

Immunoblot analysis of microsomes from rat and human brain using antiserum to hepatic P-450 1a

Immunoblot analysis of rat brain microsomal proteins using antiserum to P-450 1a1 showed the constitutive presence of P-450 1a in different regions of rat brain (Fig. 4a). Similar immunoblot studies were carried out using microsomes prepared from human brain regions obtained at autopsy (Fig. 4b). The constitutive presence of P-450 1A1 was detectable in all the human brain regions examined. An immunoreactive protein of molecular weight approximately 55 kDa was detectable in microsomes prepared from various regions of human brains such as cortex, cerebellum, striatum, and hippocampus. Another band of slightly lower molecular weight was also seen in both rat and human brain. This band could represent P-450 1a2/1A2 or a proteolytic product of P-450 1a1/1A1.

Immunohistochemical localization of P-450 1a1 in rat brain

Immunohistochemical studies demonstrated the presence of P-450 1a1 protein predominantly in neuronal cells in rat brain. A higher magnification of cortical neurons in rat brain showing the expression of P-450 1a1 is depicted in Fig. 5(a). Intense labeling of apical dendrites was observed in cortical neurons. Staining of Purkinje and granular cells was observed when sections were incubated with antiserum P-450 1a1 (Fig. 5b). Expression of P-450 1a1 was also seen in midbrain reticular neurons. Intense immunostaining was seen in apical neurites of reticular neurons (Fig. 5c). The neurons in the olfactory glomeruli were intensely stained (Fig. 5d). Immunostaining was observed in CA1 pyramidal

Fig. 6 Immunohistochemical localization of P-450 1A1 in human brain frontal cortex and midbrain using antiserum to P-450 1a1. (a) Intense immunolabeling of neurons in frontal cortex was seen indicating the presence of P-450 1A1. The apical dendrites were also stained. Bar = 10 μm. (b) Immunostaining of reticular neurons in the midbrain indicating the presence of P-450 1A1 observed. Bar = 10 μm. (c) Localization of P-450 1A1 in the granule cells (arrowhead) and Purkinje cell (double arrow) is depicted. Bar = 10 μm. (d) Immunostaining of CA1 pyramidal neurons indicating the presence of P-450 1A1. Bar = 10 μm. (e) No staining was seen in cerebral cortex section incubated with non-immune serum. Bar = 100 μm. (f) A similar section of midbrain treated with non-immune serum did not show immunostaining. Bar = 100 μm. (g) Control section incubated with non-immune serum did not show immunostaining in the cerebellum. Bar = 100 μm. (h) Similar section treated with non-immune serum did not show immunostaining of the CA1 neurons. Bar = 100 μm.

neurons of hippocampus (Fig. 5e) showing the presence of P-450 1a1 in rat brain. The neurites of CA1 neurons were intensely labelled. P-450 1a1 expression was also seen in neurons of the anteroventral nucleus of thalamus (Fig. 5f). Intense immunostaining was observed in striatal neurons, indicating the presence of P-450 1a1 protein (Fig. 5g). Intense staining of anterior horn cells in spinal cord demonstrated the expression of P-450 1a1 (Fig. 5h), whereas similar sections pre-treated with non-immune serum did not show any staining (Figs 5i–l).

Localization of P-450 1A1 in human brain

Immunohistochemical analysis using antiserum to rat liver P-450 1a1 demonstrated the predominant presence of P-450 1A1 in a neuronal population in human brain in concordance with *in situ* experiments. Intense staining of the neuronal cell body and apical dendrites was seen in frontal cortex (Fig. 6a). Reticular neurons of the midbrain (Fig. 6b) were also intensely immunostained. Similar sections incubated with non-immune serum did not show any staining (Figs 6e and f). In the cerebellum, granule cells and Purkinje cells were stained (Fig. 6c), with the granule cells being more intensely stained compared to Purkinje cells. The CA1 neurons in the hippocampus were also stained although less intensely than in the cerebellum (Fig. 6d).

RT–PCR analysis of RNA from rat and human brain cortex

RT–PCR analysis of the cDNA prepared from human brain RNA from 13 subjects, yielded a 305-bp fragment instead of the expected 392-bp product, indicating the presence of a splice variant of CYP1A1 in human brain (Fig. 7a). The sequencing of the RT–PCR product revealed complete sequence identity with CYP1A1 in the amplified region except that it lacked exon 6. We were able to amplify brain and liver RNA from the same individual. The exon 6 deleted RT–PCR product (305 bp) was detected only in the brain; the amplicon from liver RNA yielded a product of having 392 bp, indicating the presence of exon 6 (Fig. 7b). Thus, the unique splice variant having exon 6 deletion is present only in the brain and not in the liver from the same individual. Amplification of the same region of the rat brain and liver Cyp1a1 yielded a 554-bp product, which was the expected size indicating that exon 6 was intact in Cyp1a1 gene in both rat brain and liver (Fig. 7c).

3D structure modeling

In order to evaluate the potential differences in the active site and/or substrate access channel, P-450 1A1 and P-450 1A1 variant structural models were compared. Both models were prepared with the program MODELLER using the P-450 2C5 template coordinates bound to DMZ. The alignment used is shown in Fig. 8, and followed that of Szklarz and

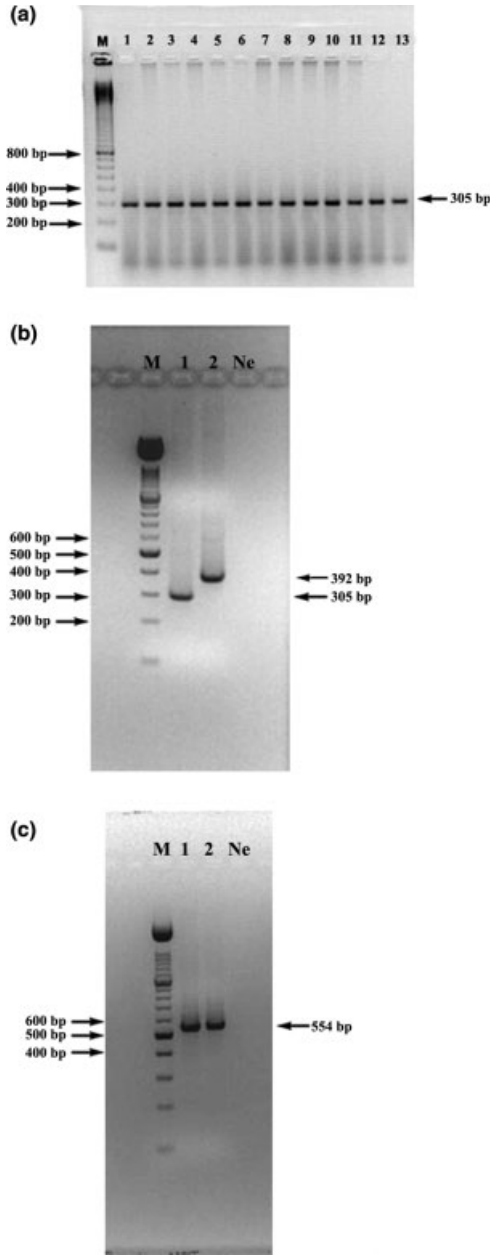

Fig. 7 RT–PCR amplification of cyp1a1 and CYP1A1 in rat and human brain. (a) Total RNA was extracted from autopsy human brain samples and RT–PCR reaction was carried out using primers specific to human liver CYP1A1. PCR amplified DNA was separated by agarose gel electrophoresis and stained with ethidium bromide. Exons 3–7 of the CYP1A1 gene was amplified by RT–PCR in 13 samples of human brain cortex obtained at autopsy. An amplicon of 305 bp was detected in all the samples indicating the deletion of exon 6. (b) RT–PCR amplification of exons 3–7 using RNA from liver (lane 2) and cerebral cortex (lane 1) from the same individual resulted in two different products having 392 and 305 bp, respectively. (c) Exons 3–7 of the *Cyp1a1* gene was amplified by RT–PCR using RNA from rat brain (lane 1) and liver (lane 2). An amplicon of 554 bp was detected in both the samples indicating the presence of exon 6. 'M' indicates molecular weight markers. 'Ne' indicates negative control.

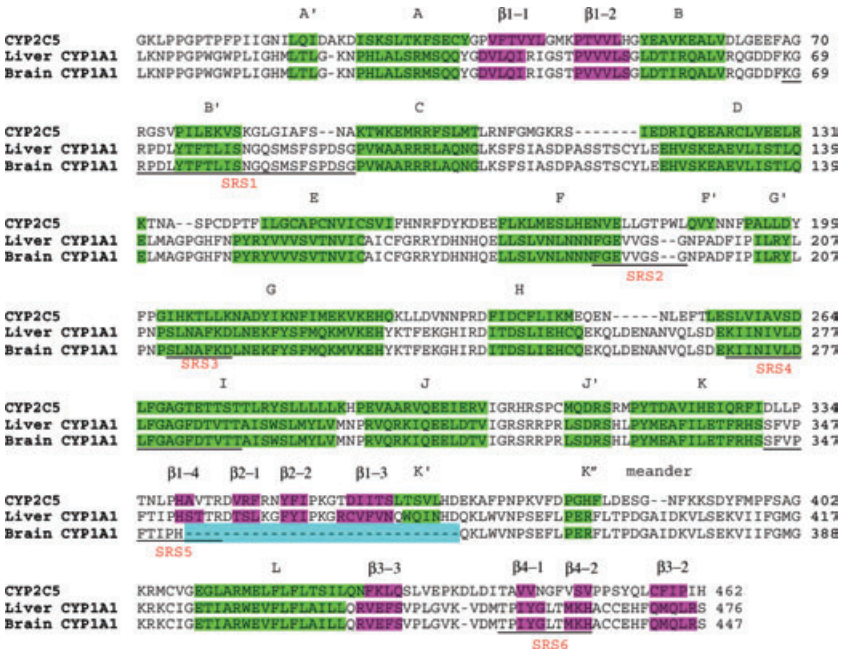

Fig. 8 Amino acid sequence alignment of CYP2C5, CYP1A1, and brain variant CYP1A1. The secondary structural elements are shown as α-helices (green highlights) and α-sheets (purple highlights). Substrate recognition sites 1–6 (SRS) are represented by underlines.

Paulsen (2002) for P-450 1A1. Figure 9 demonstrates the quality of the final models showing plots of the distance variation between the Cα carbons of the homology models and those of the P-450 2C5 template coordinates using PROFIT (http://www.bioinf.org.uk/software/profit/) The fitting in PROFIT uses the McLachlan algorithm (McLachlan 1982). The graphs show typical variances in coordinates based on the identity and similarity between the query sequences and the template. The overall Cα carbon RMSD PROFIT calculation based on the alignment in Fig. 8 of P-450 2C5 versus P-450 1A1 and brain variant P-450 1A1 was 2.21 and 2.97. The structure near the active site and substrate access channel of human brain variant P-450 1A1 appears considerably different from the well-characterized hepatic P-450 1A1 as shown in Fig. 10(a). One major structural difference noticed lies in the main substrate access channel, which has been defined as being lined by the loop between the F and G helices, β-sheets 1 and 4, and the B′ helix through X-ray crystal studies of bacterial P-450s (Peterson and Graham-Lorence 1995). This channel appears to have shifted in the human brain variant P-450 1A1 as compared to that in P-450 1A1, probably due to a compensatory effect of the protein trying to fill in the void created by the deletion (Fig. 10a). This movement of the substrate access channel could consequently alter the approach angle for substrate to the active site. The substrate access channel itself in the human brain variant P-450 1A1 appears widened. Further, the substrate binding sites, including SRS5 and SRS6, appear more open in the variant (Fig. 10b), which may allow it to accommodate larger and not so restrictive substrates like polyaromatic hydrocarbons that are typical P-450 1A1 substrates. A comparison of the structure of the loops adjacent to the deleted regions liver and brain variant of P-450 1A1 is depicted in Fig. 11. These loops provide the flexibility to allow H352 and Q382 (Q353 in brain variant) to come into the general vicinity of one another without large structural consequences in the brain variant where S353-D381 is missing.

Discussion

The constitutive expression of CYP1A1 in rat and human brain has been demonstrated by RT–PCR amplification of selected regions in the *CYP1A1* gene (Hodgson *et al*. 1993; Schilter and Omiecinski 1993; Geng and Strobel 1997; Yun *et al*. 1998; McFayden *et al*. 1998). In the present study, we demonstrate constitutive expression of full-length mRNA transcript of approximately 1.6 kb by northern blot analysis using mRNA from rat and human brain cortex (Figs 1a and b) and thus provide the first evidence for the expression of full-length mRNA of CYP1A1 in rat and human brain. Due to autolytic changes that occur during post-mortem delay, there was partial degradation of RNA as seen from the presence of lower molecular weight products in northern blot of human brain cortex from the two subjects. However, despite this, substantial expression of CYP1A1 mRNA was detectable in the northern blots performed using poly-(A^+) RNA from autopsy tissue (Fig. 1b). Earlier studies from our laboratory have demonstrated that the integrity of mRNA and protein in brain is maintained to a large extent when tissues are obtained within 12 h of post-mortem delay (Chinta *et al*. 2002).

Localization of constitutively expressed CYP1A1 in rat and human brain using FISH demonstrates the differential

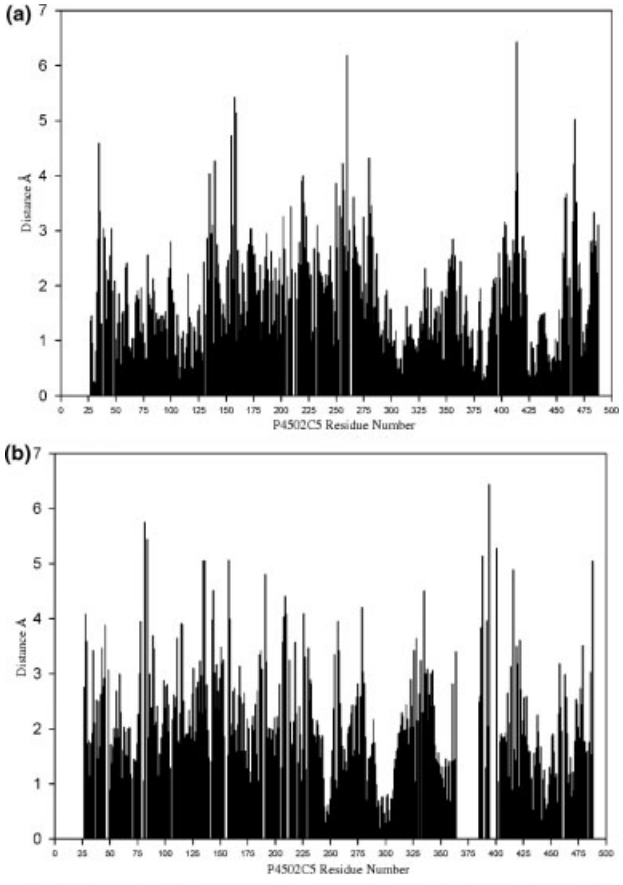

Fig. 9 Distance variation in Cα backbone position in (a) P-450 2C5 (1 N6B) versus P-450 1A1 liver model and (b) P-450 2C5 (1 N6B) versus P-450 1A1 brain variant model. PROFIT was used to give a by-residue distance difference analysis from the least squares fit of the two models compared to the template P-450 2C5 coordinates used to generate the models. The zones used for initializing the superimposition were supplied from the alignment in Fig. 8 and fitted based on Cα carbons. The overall Cα carbon RMSDs were 2.051 Å and 2.354 Å for liver and brain variant P-450 1A1, respectively. The abscissa represents the P-450 2C5 residue number. The P-450 2C5 residue numbers without a corresponding Cα carbon in liver or brain variant P-450 1A1 are seen as breaks in the data, which essentially depicts gaps in the structural alignment.

expression of CYP1A1 mRNA in different regions of brain. Throughout the brain, intense cytosolic fluorescence was observed in specific subtypes of neuronal cells such as the cortical neurons, pyramidal neurons of hippocampus, granule cell layer of the dentate gyrus, Purkinje cells of the cerebellum, reticular neurons of midbrain. While specific cell populations such as Purkinje and granule cells were labeled in the cerebellum, the cells in the molecular layer did not show any evidence for the presence of CYP1A1 or Cyp1a1. The presence of CYP1A1 in selective cell types is of interest, particularly because CYP1A1 and Cyp1a1 are induced by exposure to polycyclic aromatic hydrocarbons, which can cross the blood–brain barrier. Thus, the predominant expression of CYP1A1 in neurons, especially pyramidal neurons of hippocampus in both rat and human brain, is of special interest, as P-450 1A1 can generate reactive oxygen species, such as superoxide anion, hydroxyl radical, and hydrogen peroxide (Liu *et al*. 2001); and hippocampal neurons are especially vulnerable to oxidative stress-mediated injury such as that seen during reperfusion following cerebral ischemia (Shivakumar *et al*. 1995). Because hippocampus plays an important role in cognitive functions, such as learning and memory, damage to this area of the brain could potentially have serious consequences in humans.

Immunoblot analysis of microsomes from various regions of rat and human brain showed expression of P-450 1A1 immunoreactive protein, indicating the constitutive expression of P-450 1A1 protein in brain. These results are in agreement with our earlier reports (Anandatheerthavarada *et al*. 1990) and those from other laboratories (Kapitulnik *et al*. 1987; Kohler *et al*. 1988; Geng and Strobel 1997) but in contrast to the reports from some laboratories where they were unable to detect the Cyp1a1 protein in rat brain (Morse *et al*. 1998). Recently, Huang *et al*. (2000) have also demonstrated the constitutive expression of Cyp1a1 in the rat CNS by RT–PCR. These studies also showed the induction of Cyp1a1 by tetrachlorobenzo-p-dioxin in hypothalamus, hippocampus, cortex, cerebellum, and substantia nigra in rat brain. The subcellular localization of CYP1A1 mRNA and its role in the metabolism of the intravenous anesthetic agent propofol was also reported in human brain (Zhang *et al*. 2001). The present study for the first time demonstrates the simultaneous detection of CYP1A1 mRNA and protein using *in situ* hybridization and immunohistochemistry in neuronal cell populations. Localization of CYP1A1 predominantly in the neurons as seen in the present study may have adverse effects in terms of bioactivation of procarcinogens into reactive metabolites and increase in the generation of reactive oxygen species, which may cause oxidative damage in the brain.

RT–PCR amplification of the CYP1A1 gene using total RNA from 13 human brain autopsy samples yielded a fragment of 305 bp instead of the expected 392 bp (Fig. 7a). The human *CYP1A1* gene has a total of seven exons, of which we amplified exons 3–7. The sequencing of the RT–PCR-amplified product showed complete loss of exon 6, while the rest of the sequence had 100% identity with the human *CYP1A1* gene. All the 13 human brain samples tested showed loss of exon 6 of the *CYP1A1* gene. However, a larger number of samples need to be tested to determine if the loss of exon 6 is a common feature of the CYP1A1 enzyme in human brain. Interestingly, the splice variant was detected only in the brain but not in the liver from the same individual. P-450 levels in brain and liver are altered differentially during post-mortem delay (Chinta *et al*. 2002), therefore it is difficult to quantitate the relative abundance of the transcript in liver and

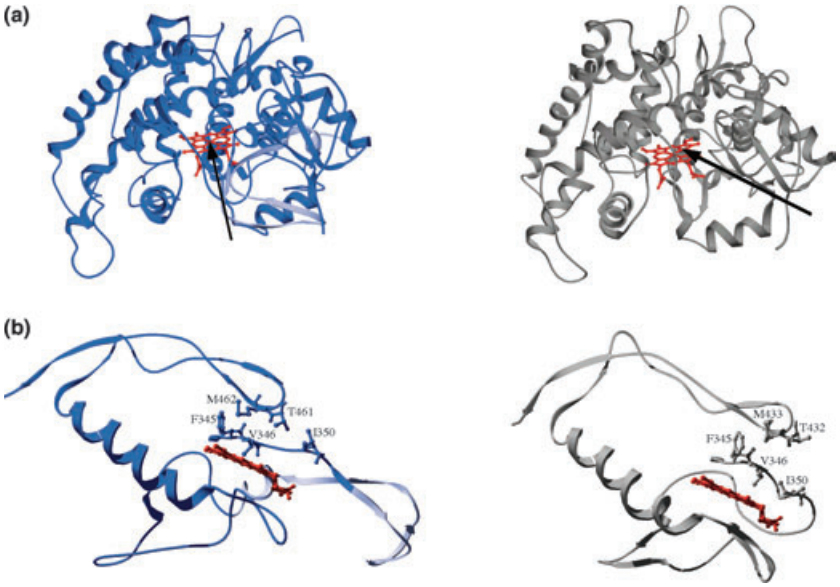

Fig. 10 3D homology modeling of CYP1A1 and CYP1A1 brain variant. Comparison between CYP1A1 liver form structure (blue) and CYP1A1 brain variant (gray). A homology model of CYP1A1 and the brain variant was constructed based on the crystal structure coordinates of mammalian P-450 2C5 complexed to sulfaphenazole. These models generated by MODELLER were superimposed to give the exact same viewing angle in both proteins with respect to the heme (red). The light blue regions denote the area deleted on CYP1A1 variant. (a) There is a remarkable movement of the substrate access channel in the variant compared to CYP1A1. This structural perturbation in the variant may alter the accessibility of substrates to the active site. Arrow represents direction of access channel. (b) This region of the active site shows CYP1A1 more compact over the heme, whereas the variant appears more relaxed. SRS5 is represented by F345, V346, I350, and SRS6 by T461 and M462. Further, this variant may be adapted to accommodate a wider range of substrates (i.e. nonplanar compounds).

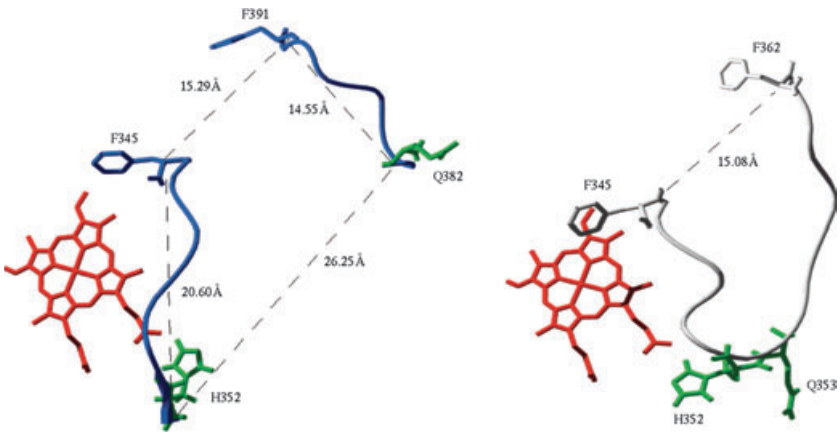

Fig. 11 Deleted region comparison of liver and brain variant P-450 1A1.The liver form is shown in blue and brain variant in gray with heme shown in red. The deleted region is removed in the liver form for clarity. Therefore, only the loops adjacent to the deletion are represented in liver P-450 1A1 and the corresponding residues are displayed for the brain variant to provide a comparison between these two proteins. F345 marks the first amino acid of the loop after the K helix and H352 (green) is the last amino acid before the deletion. Q382 (Q353 in brain variant), shown in green, to F391 (F362 in brain variant) make up the loop after the deletion, which is attached to the K′ helix.

brain from the same individual as liver P-450 levels decrease more rapidly by autolytic cleavage during post-mortem delay compared to brain P-450.

The nervous system has a propensity for generating alternate spliced forms, and splicing defects may not be related to differences in the genomic sequence but may be regulated by mechanisms involving the spliceosomal complex and RNA binding proteins, which are poorly understood (Grabowski and Black 2001). The tendency for human brain to generate alternate spliced genes as seen in the present

study wherein an alternate spliced variant having exon 6 deletion was identified only in the human brain. Human brain-specific alternate spliced forms of P-450 2D enzymes are expressed, which mediate biotransformation of drugs by pathways that are different from those seen in liver (Pai *et al*. 2004). Presumably other brain-specific alternatively spliced P-450 enzymes may be expressed in human brain, which are yet to be identified. In rat brain and liver, amplification of the same region did not reveal the presence of the alternate spliced product with exon 6 deletion, indicating that the alternate spliced product with exon 6 deletion is present only in human brain.

The deletion of exon 6 in CYP1A1 does not lead to premature termination; presumably, its translation would lead to a functional P-450 enzyme. Examination of the sequence of the RT–PCR product, especially at the beginning of exon 7, indicates that there is no frame shift as compared to CYP1A1. The structural modeling of the putative protein indicates that there would be alteration in the substrate access channel possibly allowing for less restricted access and altered angle of approach as compared to the normal CYP1A1. The deleted region begins within the α1–4 sheet and extends through the K′-K′ loop. It seems reasonable that the variant could withstand this deletion without causing a complete change in the overall structure compared to liver P-450 1A1 given the positioning of the two residues flanking the deletion. A comparison of the liver and brain variant forms surrounding and including this region is shown in Fig. 11. However, as noted in the alignment in Fig. 8, the deletion includes one side of the substrate access channel, α1–4 and 1–3 sheets, and also a portion of substrate recognition site 5. Therefore, the possibility of this deletion causing substantial changes in substrate preference due to its location should be noted despite not having large global conformational differences from liver P-450 1A1. Noble *et al*. (1999) have shown in P-450 BM3 that a mutation from Phe4 2 > Ala lining the substrate access channel proved to increase the K_m for two different substrates. This shows importance of volume considerations in substrate access through the channel. The same type of results may occur for the P-450 1A1 human brain variant as compared to the P-450 1A1 liver form as the access channel appears broader in the variant. Therefore, K_s and K_m values for the P-450 1A1 variant should decrease as compared to P-450 1A1. A broader substrate access channel would also allow for more free movement of the substrate within the access channel, which could likely lead to the formation of more than one metabolite. P-450 1A1 is one of very few P-450 enzymes with a high degree of preference for flat planar molecules as substrates; for example, polyaromatic hydrocarbons. Size of the active site, character of the substrate access channel, and angle of approach are among the characteristics, which establish substrate preference. As cited in the Results section, these characteristics appear altered in the P-450 1A1 variant such that the variant may be more suited to substrates other than flat planar molecules. Our modeling studies confirm that a portion of SRS5 is absent and the residues approximating the position of SRS5 in hepatic P-450 1A1 are non-analagous, supporting the prediction of a less restrictive active site. The current models suggest candidate sites or residue mutations to evaluate the role of SRS5 in substrate binding. Further, replacing the missing stretch with non-homologous polypeptides may allow us to evaluate the specificity or non-specificity of chain composition in the substrate access channel or size of the active site. The cloning and expression of this variant, subsequent generation of mutants, and binding/kinetic studies currently in progress would help address the above and further refine the 3D homology models.

In conclusion, the study demonstrates the presence of alternate spliced forms of P-450 in human brain. The presence of as yet unidentified P-450 enzymes generated by alternate splicing would help understand the specific biotransformation pathways occurring at the target site of action of drugs.

Acknowledgements

We thank Prof. S. K. Shankar for providing the human brain samples through the Human Brain Tissue Repository at Department of Neuropathology, NIMHANS, Bangalore. The technical assistance of Mr V. K. Prasanna is acknowledged. National Institutes of Health grant MH55494 supported this research.

References

Anandatheerthavarada H. K., Shankar S. K. and Ravindranath V. (1990) Rat brain cytochromes P-450: catalytic, immunochemical properties and inducibility of multiple forms. *Brain Res.* **536**, 339–343.

Bradford M. M. (1976) A rapid and sensitive method for the quantitation of microgram quantities of protein utilizing the principle of dye-binding. *Anal. Biochem.* **72**, 248–254.

Chinta S. J., Pai H. V., Upadhya S. C., Boyd M. R. and Ravindranath V. (2002) Constitutive expression and localization of the major drug metabolizing enzyme, cytochrome P-450 2D in human brain. *Mol. Brain Res.* **103**, 49–61.

Chomezynski P. (1993) A reagent for the single-step simultaneous isolation of RNA, DNA and protein from cell and tissue samples. *Biotechniques* **15**, 532–537.

Farin F. M. and Omiecinski C. J. (1993) Regio-specific expression of cytochrome P-450s and microsomal epoxide hydrolase in human brain tissue. *J. Toxicol. Environ. Health* **40**, 317–335.

Geng J. and Strobel H. W. (1997) Expression and induction of cytochrome P-450 1A1 and P-450 2D subfamily in the rat glioma C6 cell line. *Brain Res.* **774**, 11–19.

Glowinski J. and Iversen L. L. (1966) Regional studies of catecholamines in the rat brain. I. The disposition of [^{3}H] norepinephrine, [^{3}H] dopamine and [^{3}H] dopa in various regions of the brain. *J. Neurochem.* **13**, 655–669.

Gozukara E. M., Fagan J., Pastewka J. V., Guengerich F. P. and Gelboin H. V. (1984) Induction of cytochrome P-450 mRNAs quantitated by *in vitro* translation and immunoprecipitation. *Arch. Biochem. Biophys.* **232**, 660–669.

Grabowski P. J. and Black D. L. (2001) Alternative RNA splicing in the nervous system. *Prog. Neurobiol.* **65**, 289–308.

Gram T. E., Okine L. K. and Gram R. A. (1986) The metabolism of xenobiotics by certain extrahepatic organs and its relation to toxicity. *Annu. Rev. Pharmacol. Toxicol.* **26**, 259–291.

Guex N. and Peitsch M. C. (1997) SWISS-MODEL and the Swiss-PdbViewer: an environment for comparative protein modeling. *Electrophoresis* **18**, 2714–2723.

Hodgson A. V., White T. B., White J. W. and Strobel H. W. (1993) Expression analysis of the mixed function oxidase system in rat brain by the polymerase chain reaction. *Mol. Cell. Biochem.* **120**, 171–179.

Huang P., Rannug A., Ahlbom E., Hakansson H. and Ceccatelli S. (2000) Effect of 2,3,7,8-Tetrachlorodibenzo-p-dioxin on the expression of cytochrome P-450 1A1, the Aryl hydrocarbon receptor, and the Aryl hydrocarbon receptor nuclear translocator in rat brain and pituitary. *Toxicol. Appl. Pharmacol.* **169**, 159–167.

Humphrey W., Dalke A. and Schulten K. (1996) VMD: visual molecular dynamics. *J. Mol. Graphics* **14**, 33–38.

Jones P. B., Durrin L. K., Fisher J. M. and Whitlock J. P. Jr (1986) Control of gene expression by 2,3,7,8-tetrachlorodibenzo-p-dioxin. Multiple dioxin-responsive domains 5′-ward of the cytochrome P1–450 gene. *J. Biol. Chem.* **261**, 6647–6650.

Kalé L., Skeel R., Bhandarkar M. *et al.* (1999) NAMD2: greater scalability for parallel molecular dynamics. *J. Computat. Physics* **151**, 283–312.

Kapitulnik J., Gelboin H. V., Guengerich F. P. and Jacobowitz D. M. (1987) Immunohistochemical localization of cytochrome P-450 in rat brain. *Neuroscience* **20**, 829–833.

Kevil C. G., Walsh L., Laroux F. S., Kalogeris T., Grisham M. B. and Alexander J. S. (1997) An improved, rapid northern protocol. *Biochem. Biophys. Res. Commun.* **238**, 277–279.

Kohler C., Eriksson L. G., Hansson T., Warner M. and Ake-Gustafsson J. (1988) Immunohistochemical localization of cytochrome P-450 in rat brain. *Neurosci. Lett.* **84**, 109–114.

Laemmli U. K. and Favre M. (1973) Maturation of the head of bacteriophage T4. I. DNA packaging events. *J. Mol. Biol.* **80**, 575–599.

Laskowski R. A., MacArthur M. W., Moss D. S. and Thornton J. M. (1993) PROCHECK: a program to check the stereochemical quality of protein structures. *J. Appl. Cryst.* **26**, 283–291.

Liu L., Bridges R. J. and Eyer C. L. (2001) Effect of cytochrome P-450, 1A induction on oxidative damage in rat brain. *Mol. Cell. Biochem.* **223**, 89–94.

McFayden M. C., Melvin W. T. and Murray G. I. (1998) Regional distribution of individual forms of cytochrome P-450 mRNA in normal adult human brain. *Biochem. Pharmacol.* **55**, 825–830.

McLachlan A. D. (1982) Rapid comparison of protein structures. *Acta Cryst.* **A38**, 871–873.

de Montellano M. (1986) *Cytochrome P-450: Structure, Mechanism and Biochemistry.* Plenum Press, New York.

Morse D. C., Stein A. P., Thomas P. E. and Lowndes H. E. (1998) Distribution and induction of cytochrome P450 1A1 and 1A2 in rat brain. *Toxicol. Appl. Pharmacol.* **152**, 232–239.

Noble M. A., Miles C. S., Chapman S. K., Lysek D. A., MacKay A. C., Reid G. A., Hanzlik R. P. and Munro A. W. (1999) Roles of key active-site residues in flavocytochrome P450 BM3. *Biochem. J.* **339**, 371–379.

Pai H. V., Kommaddi R. P., Chinta S. J., Mori T., Boyd M. R. and Ravindranath V. (2004) A frame shift mutation and alternate splicing generates a functional isoform of the pseudogene, cytochrome P4502D7 in human brain that demethylates codeine to morphine. *J. Biol. Chem.* **279**, 27 383–27 389.

Park J. Y., Shigenaga M. K. and Ames B. N. (1996) Induction of cytochrome P-450 1A1 by 2,3,7,8-tetrachlorodibenzo-p-dioxin or indolo (3,2-b) carbazole is associated with oxidative DNA damage. *Proc. Natl Acad. Sci. USA* **93**, 2322–2327.

Peterson J. A. and Graham-Lorence S. E. (1995) In: *Bacterial P-450s Structural Similarities and Functional Differences* (Ortiz de Montellano, P. R., eds), pp. 652. Plenum Press, New York.

Ravindranath V. and Anandatheerthavarada H. K. (1990) Preparation of brain microsomes with cytochrome P-450 activity using calcium aggregation method. *Anal. Biochem.* **187**, 310–313.

Ravindranath V. and Boyd M. R. (1995) Xenobiotic metabolism in brain. *Drug Metab. Rev.* **27**, 419–448.

Ravindranath V., Anandatheerthavarada H. K. and Shankar S. K. (1989) Xenobiotic metabolism in human brain: presence of cytochrome P-450 and associated mono-oxygenases in human brain regions. *Brain Res.* **496**, 331–335.

Sali A. and Blundell T. L. (1993) Comparative protein modelling by satisfaction of spatial restraints. *J. Mol. Biol.* **234**, 779–815.

Schilter B. and Omiecinski C. J. (1993) Regional distribution and expression modulation of cytochrome P-450 and epoxide hydrolase mRNAs in the rat brain. *Mol. Pharmacol.* **44**, 990–996.

Shivakumar B. R., Kolluri S. V. and Ravindranath V. (1995) Glutathione and protein thiol homeostasis in brain during reperfusion after cerebral ischemia. *J. Pharmacol. Exp. Ther.* **274**, 1167–1173.

Strolin-Benedetti M., Brogin G., Bani M., Oesch F. and Hengstler J. G. (1999) Association of cytochrome P-450 induction with oxidative stress *in vivo* as evidenced by 3-hydroxylation of salicylate. *Xenobiotica* **29**, 1171–1180.

Szklarz G. D. and Paulsen M. D. (2002) Molecular modeling of cytochrome P-450 1A1: enzyme–substrate interactions and substrate binding affinities. *J. Biomol. Struct. Dyn.* **20**, 155–162.

Towbin T., Staehelin J. and Gordon J. (1979) Electrophoretic transfer of proteins from polyacrylamide gels to nitrocellulose sheets: procedure and some applications. *Proc. Natl Acad. Sci. USA* **76**, 4350–4354.

Wester M. R., Johnson E. F., Marques-Soares C., Dansette P. M., Mansuy. D. and Stout C. D. (2003) Structure of a substrate complex of mammalian cytochrome P-450 2C5 at 2.3 Å resolution: evidence for multiple substrate binding modes. *Biochemistry* **42**, 6370–6379.

Yun C. H., Park H. J., Kim S. J. and Kim H. K. (1998) Identification of cytochrome P-450 1A1 in human brain. *Biochem. Biophys. Res. Commun.* **243**, 808–810.

Zhang S. H., Li Q., Yao S. L. and Zeng B. X. (2001) Subcellular expression of UGT1A6 and CYP1A1 responsible for propofol metabolism in human brain. *Acta Pharmacol. Sin.* **22**, 1013–1017.